

Improved bending property of half-filled photonic crystal fiber

Yiping Wang,^{1,2,3,*} Xiaoling Tan,¹ Wei Jin,¹ Shujing Liu,¹ Diqing Ying,¹ and Yeuk Lai Hoo¹

¹Department of Electrical Engineering, The Hong Kong Polytechnic University, Kowloon Hong Kong, China

²Optoelectronics Research Centre, University of Southampton, Southampton SO17 1BJ, U.K.

³Photonic Research Center, Harbin Engineering University, Harbin 150001, China.

*ypwang@china.com

Abstract: A half-filling technique was demonstrated to improve the bending properties of a fluid-filled photonic crystal fiber. Such a technique can realize to fill selectively a fluid into half of air holes in a PCF. The bending properties of the half-filled PCF are quite different from those of the fully-filled PCF. Distinct bending properties were observed when the half-filled PCF was bent toward different fiber orientations. Especially, the transmission spectrum of the half-filled PCF was hardly affected while the fiber was bent toward the filled-hole orientation.

©2010 Optical Society of America

OCIS codes: (060.4005) Microstructured fibers; (060.5295) Photonic crystal fibers.

References and links

1. B. J. Eggleton, C. Kerbage, P. S. Westbrook, R. S. Windeler, and A. Hale, "Microstructured optical fiber devices," *Opt. Express* **9**(13), 698–713 (2001).
2. R. T. Bise, R. S. Windeler, K. S. Kranz, C. Kerbage, B. J. Eggleton, and D. J. Trevor, "Tunable photonic band gap fiber," in *Optical Fiber Communication Conference and Exhibit*, Vol. 70 of OSA Trends in Optics and Photonics (Optical Society of America, 2002) 466–468 (2002).
3. Y. Wang, X. Tan, W. Jin, D. Ying, Y. L. Hoo, and S. Liu, "Temperature-controlled transformation in fiber types of fluid-filled photonic crystal fibers and applications," *Opt. Lett.* **35**(1), 88–90 (2010).
4. J. Lægsgaard, and T. T. Alkeskjold, "Designing a photonic bandgap fiber for thermo-optic switching," *J. Opt. Soc. Am. B* **23**(5), 951–957 (2006).
5. T. Larsen, A. Bjarklev, D. Hermann, and J. Broeng, "Optical devices based on liquid crystal photonic bandgap fibres," *Opt. Express* **11**(20), 2589–2596 (2003).
6. Y. Wang, W. Jin, L. Jin, X. Tan, H. Bartelt, W. Ecke, K. Moerl, K. Schroeder, R. Spittel, R. Willsch, J. Kobelke, M. Rothhardt, L. Shan, and S. Brueckner, "Optical switch based on a fluid-filled photonic crystal fiber Bragg grating," *Opt. Lett.* **34**(23), 3683–3685 (2009).
7. Y. Wang, H. Bartelt, W. Ecke, K. Moerl, H. Lehmann, K. Schroeder, R. Willsch, J. Kobelke, M. Rothhardt, R. Spittel, L. Shan, S. Brueckner, W. Jin, X. Tan, and L. Jin, "Thermo-optic switching effect based on fluid-filled photonic crystal fiber," *IEEE Photon. Technol. Lett.* **22**(3), 164–166 (2010).
8. P. Steinvurzel, E. D. Moore, E. C. Mägi, and B. J. Eggleton, "Tuning properties of long period gratings in photonic bandgap fibers," *Opt. Lett.* **31**(14), 2103–2105 (2006).
9. T. B. Iredale, P. Steinvurzel, and B. J. Eggleton, "Electric-arc-induced long-period gratings in fluid-filled photonic bandgap fibre," *Electron. Lett.* **42**(13), 739–740 (2006).
10. C. Kerbage, A. Hale, A. Yablon, R. S. Windeler, and B. J. Eggleton, "Integrated all-fiber variable attenuator based on hybrid microstructure fiber," *Appl. Phys. Lett.* **79**(19), 3191–3193 (2001).
11. C.-P. Yu, J.-H. Liou, S.-S. Huang, and H.-C. Chang, "Tunable dual-core liquid-filled photonic crystal fibers for dispersion compensation," *Opt. Express* **16**(7), 4443–4451 (2008).
12. A. Sharkawy, D. Pustai, S. Shi, D. Prather, S. McBride, and P. Zanzucchi, "Modulating dispersion properties of low index photonic crystal structures using microfluidics," *Opt. Express* **13**(8), 2814–2827 (2005).
13. T. A. Birks, F. Luan, G. J. Pearce, A. Wang, J. C. Knight, and D. M. Bird, "Bend loss in all-solid bandgap fibres," *Opt. Express* **14**(12), 5688–5698 (2006).
14. A. Argyros, T. Birks, S. Leon-Saval, C. M. B. Cordeiro, and P. St J Russell, "Guidance properties of low-contrast photonic bandgap fibres," *Opt. Express* **13**(7), 2503–2511 (2005).
15. G. Ren, P. Shum, L. Zhang, M. Yan, X. Yu, W. Tong, and J. Luo, "Design of all-solid bandgap fiber with improved confinement and bend losses," *IEEE Photon. Technol. Lett.* **18**(24), 2560–2562 (2006).
16. T. Muraio, K. Saitoh, and M. Koshiba, "Detailed theoretical investigation of bending properties in solid-core photonic bandgap fibers," *Opt. Express* **17**(9), 7615–7629 (2009).
17. C. Kerbage, P. Steinvurzel, P. Reyes, P. S. Westbrook, R. S. Windeler, A. Hale, and B. J. Eggleton, "Highly tunable birefringent microstructured optical fiber," *Opt. Lett.* **27**(10), 842–844 (2002).

18. Y. Huang, Y. Xu, and A. Yariv, "Fabrication of functional microstructured optical fibers through a selective-filling technique," *Appl. Phys. Lett.* **85**(22), 5182–5184 (2004).
19. K. Nielsen, D. Noordegraaf, T. Sorensen, A. Bjarklev, and T. P. Hansen, "Selective filling of photonic crystal fibres," *J. Opt. A, Pure Appl. Opt.* **7**(8), L13–L20 (2005).
20. B. T. Kuhlmeiy, B. J. Eggleton, and D. K. C. Wu, "Fluid-filled solid-core photonic bandgap fibers," *J. Lightwave Technol.* **27**(11), 1617–1630 (2009).
21. D. K. C. Wu, B. T. Kuhlmeiy, and B. J. Eggleton, "Ultrasensitive photonic crystal fiber refractive index sensor," *Opt. Lett.* **34**(3), 322–324 (2009).
22. S. Liu, L. Jin, W. Jin, D. Wang, C. Liao, and Y. Wang, "Structural long period gratings made by drilling micro-holes in photonic crystal fibers with a femtosecond infrared laser," *Opt. Express* **18**(6), 5496–5503 (2010).
23. Y. Wang, H. Bartelt, S. Brueckner, J. Kobelke, M. Rothhardt, K. Mörl, W. Ecke, and R. Willsch, "Splicing Ge-doped photonic crystal fibers using commercial fusion splicer with default discharge parameters," *Opt. Express* **16**(10), 7258–7263 (2008).
24. Y. Wang, W. Jin, J. Ju, H. Xuan, H. L. Ho, L. Xiao, and D. Wang, "Long period gratings in air-core photonic bandgap fibers," *Opt. Express* **16**(4), 2784–2790 (2008).
25. L. Xiao, M. S. Demokan, W. Jin, Y. Wang, and C.-L. Zhao, "Fusion splicing photonic crystal fibers and conventional single-mode fibers: microhole collapse effect," *J. Lightwave Technol.* **25**(11), 3563–3574 (2007).
26. Y. Wang, H. Bartelt, W. Ecke, R. Willsch, J. Kobelke, M. Kautz, S. Brueckner, and M. Rothhardt, "Sensing properties of fiber Bragg gratings in small-core Ge-doped photonic crystal fibers," *Opt. Commun.* **282**(6), 1129–1134 (2009).
27. L. Xiao, W. Jin, and M. S. Demokan, "Photonic crystal fibers confining light by both index-guiding and bandgap-guiding: hybrid PCFs," *Opt. Express* **15**(24), 15637–15647 (2007).
28. Y.-P. Wang, and Y.-J. Rao, "A novel long period fiber grating sensor measuring curvature and determining bend-direction simultaneously," *IEEE Sens. J.* **5**(5), 839–843 (2005).

1. Introduction

Microstructures in photonic crystal fibers (PCFs) allow advanced materials to be filled into their air holes, offering a new platform for developing innovative communication and sensing applications [1]. An index-guiding PCF could be transform into a bandgap-guiding fiber by means of filling a high index material into the air holes [2,3]. Such a transformation in the fiber types may lead to various promising devices such as optical switches [4–7], tunable filters [8,9], attenuators [10], and dispersion compensators [11,12]. Compared with the index-guiding pure-silica PCFs, the bandgap-guiding fluid-filled PCFs are more susceptible to bend due to the low effective index mismatch between the fluid rod and the background silica [13–16]. As a result, the bandgaps of the fluid-filled PCFs could obviously be changed, even disappear, with the decrease of the bend radius. Such a bend-induced change of the bandgaps will result in bit error rate soaring in a practical communication system. Unique optical properties could be achieved by selectively filling a fluid into the air holes of a PCF [17–21]. A selective filling technique based on the dependence of filling speed on the size of the air holes was demonstrated in [18,19]. Such a technique cannot, however, realize to fill selectively the air holes with same sizes. Another one is direct manual gluing technique, allowing the creation of any arbitrary pattern of filled and unfilled holes [20,21].

In this letter, a half-filling technique was demonstrated to improve the bending properties of a fluid-filled PCF in which half of air holes were selectively filled. Compared with a fully-filled PCF, distinct bending properties were achieved in a half-filled PCF and strongly depend on the bending orientations of the fiber.

2. Half-filling technique of PCF

A pure-silica solid-core PCF (LMA-10 from Crystal Fiber) was employed to demonstrate our proposed technique, as shown in Fig. 1(b). First of all, as shown in Figs. 1(a1) and 1(d), a rectangular groove with a width of about 30 μm and a depth of about 55 μm was craved on the side of the PCF by the use of a micromachining system consisting of a femtosecond laser and a microscope (Nikon ECLIPSE 80i) [22]. Consequently, about half of air holes in the PCF were exposed at the grooved section. Secondly, as shown in Figs. 1(a2) and 1(e), one end of the PCF with the groove was fused into a spherical end at a distance of 5 mm from the groove to completely collapse the air holes at the fiber end by an arc discharge technique [23] or a CO_2 laser irradiation technique [24]. Another end of the PCF was spliced to a standard single-mode fiber (SMF) by an arc fusion splicing technique [23,25]. Thirdly, as shown in Fig. 1(a3),

the spherical end of the PCF with the groove was immersed into a refractive index matching liquid (Cargille Labs, $n = 1.480$, thermo-optic coefficient: $-4.15 \times 10^{-4}/^{\circ}\text{C}$). It is critical point to immerse completely the groove into the fluid. So the fluid was filled into the exposed holes of the PCFs with the well-known capillarity action. Consequently, about half of holes in the PCF were selectively filled by the fluid, as shown in Figs. 1(c) and 1(f) in which the light side of the fiber illustrates the fluid-filled holes whereas the dark side illustrates the unfilled holes. The PCF employed has a total length of 350 mm, and the half-filled PCF has actually a length of about 200 mm.

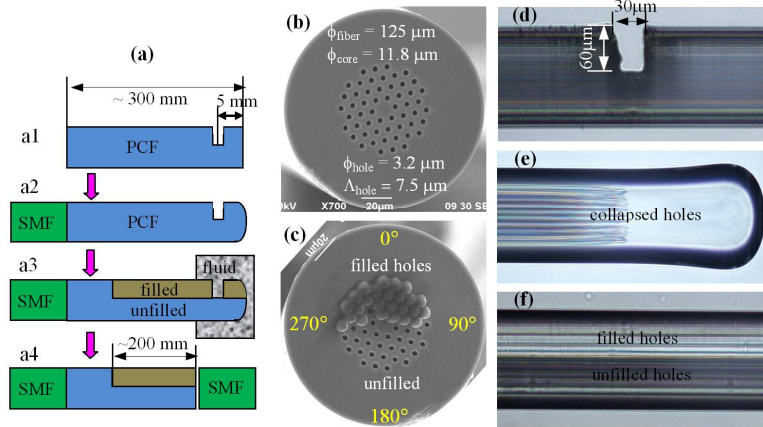


Fig. 1. (a) Schematic diagram for filling a fluid into about half of holes in the PCF; Cross-section of the (b) unfilled and (c) half-filled PCFs; Side images of (d) the grooved PCF, (e) the PCF spherical end, and (f) the half-filled PCF. (d), (e) and (f) were observed by the use of a microscope whose focal plane was adjusted to the fiber axis. In (c), the fluid overflowed on the hole ends as a result of the vacuum during scanning electron micrographs, where the ‘0°’ orientation corresponds to the direction being perpendicular to the bottom of the groove.

Finally, as shown in Fig. 1(a4), the spherical end of the half-filled PCF was cleaved to move the groove and was butt-coupled to another standard SMF to observe its transmission spectrum with a supercontinuum white light source (KOHERAS SuperK Compact) and an optical spectrum analyzer (ANDO AQ6317B). As shown in the transmission spectrum (blue curve) of the half-filled PCF in Fig. 2, three attenuation gaps were observed within the measured wavelength range. In other words, three bandgaps, gap1, gap2 and gap3, occurred respectively within the wavelength ranges, resulting from the higher index of the filled fluid rods than that of the pure-silica background in the PCF. The extinction ratio of the second bandgap near 1000 nm is as high as about 40dB. In order to investigate the function difference between the half- and fully-filled PCFs, we also filled all air holes in the same type of PCF with the same fluid and measured the transmission spectrum of the fully-filled PCF, as illustrated by the red curve in Fig. 2. It is interesting to see from Fig. 2 that the fully-filled PCF has a similar transmission spectrum as the half-filled PCF.

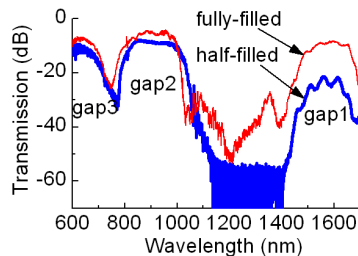


Fig. 2. Transmission spectra of the fully- and half-filled PCFs, where three bandgaps, gap1, gap2, and gap3, were observed within the measured wavelength range.

3. Bending properties of fluid-filled PCF

The bending properties of the fully- and half-filled PCFs were investigated with an experimental setup as illustrated in Fig. 3 [26]. The left end of the fiber was fixed, and the right end was moved gradually toward the left end in order to bend the PCF symmetrically. Such a bending procedure was repeated after the fiber was rotated around its axis by angles of 90°, 180° and 270°. The curvature of the bent fiber could be approximately calculated by the relation below:

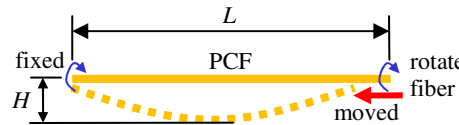
$$C = 2H / (H^2 + L^2/4) \quad (1)$$


Fig. 3. Schematic diagram of the experimental setup for measuring the bending properties of the fluid-filled PCFs.

We firstly measured the transmission spectrum evolution of the fully-filled PCF with the decrease of the bend radius (the increase of the fiber curvature). As shown in Fig. 4(a), with the decrease of the bend radius, the short-wavelength ('blue') edge of each bandgap shifted sharply toward the longer wavelength, whereas the long-wavelength ('red') edge shifted slowly toward the shorter wavelength. In other words, the bandgaps, in general, narrowed gradually with the decrease of the bend radius. Similar transmission spectrum evolutions were observed when the fully-filled PCF was bent toward different fiber orientations.

Then the bending properties of the half-filled PCF were investigated while the fiber was bent toward different fiber orientations. We marked the orientation of the groove by sticking a tag on the PCF during the groove fabrication, as shown in Fig. 1(c), in which the '0°' orientation corresponds to the direction being perpendicular to the bottom of the groove. It is interesting to see from Fig. 4 that orientation-dependent bending properties were observed when the half-filled PCF was bent toward different fiber orientation. As shown in Figs. 4(b), the transmission spectrum hardly changed while the half-filled PCF was bent toward the filled-hole side, i.e. the '0°' orientation. Whereas, while the half-filled PCF was bent toward the unfilled-hole side, i.e. the '180°' orientation (Fig. 4(e), and another two fiber orientations of '90°' (Fig. 4(c) and '270°' (Fig. 4(f), the 'blue' edge of each bandgap shifted toward the longer wavelength and the 'red' edge shifted toward the shorter wavelength.

In order to evaluate quantitatively the bend-induced shift sensitivities of the bandgap edges, Fig. 4(d) illustrates the wavelengths, corresponding to the transmission of -20 dB, at the 'blue' edge of the second bandgap for each bending sample above with increased curvature of the fiber. For the cases of the fully-filled PCF and the half-filled PCF bent toward the 0°, 90°, 180° and 270° orientations, the 'blue' edge of the second bandgap at -20dB shifted by about 135, 1, 3, 18 and 7 nm, respectively, when the curvature of the fiber was increased to 20 m⁻¹. Therefore, compared with the fully-filled PCF, the half-filled PCF has a lower bend-sensitivity and even is insensitive to the increased curvature while the fiber is bent toward the side of the fluid-filled holes. This is of advantage to the communication applications of the fluid-filled PCFs.

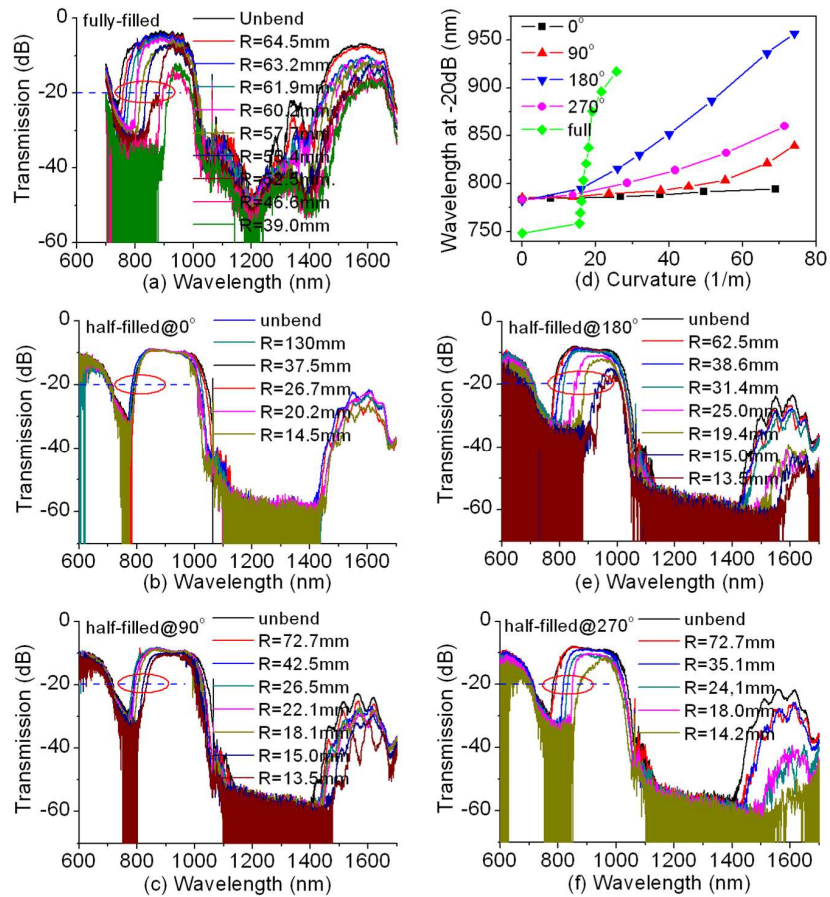


Fig. 4. Transmission spectrum evolutions of (a) the fully-filled PCF and the half-filled PCF bent toward the (b) 0°, (c) 90°, (e) 180° and (f) 270° orientations with the decrease of the bend radius; (d) Wavelengths, corresponding to the transmission of -20dB, at the 'blue' edge of the second bandgap (see 'red' circles in (a), (b), (c), (e), and (f)) with the increase of the bend curvature.

4. Discussion

In conventional glass fibres, the bend loss arises from the resonant coupling of light from the core to phase-matched radiation modes in the cladding on the outside of the bend. Moreover, a lower effective index mismatch between the fundamental and cladding modes could result in a larger bend loss in a bent fiber [13–16]. A different loss mechanism occurs in all-solid bandgap fibers in which the bend loss will arise mainly at the 'blue' or 'red' wavelength edge of the low-loss windows [15,16], depending on which of the downward and upward effective index mismatches, Δn_- and Δn_+ , is smaller [13,14]. Our fully-filled PCF may be regarded as a so-called all-solid bandgap fiber. As shown in Fig. 5, the core mode effective index (red curve) is closer to the band below than the band above over each bandgap. Hence, Δn_- is smaller than Δn_+ in our fully-filled PCF, and the shorter the wavelength is, the smaller the Δn_- is. As a result, a larger bend loss occurs at the 'blue' edge of each bandgap than at the 'red' edge. Consequently, the 'blue' edge of each bandgap shifts sharply toward the longer wavelength with the decrease of the bend radius, whereas the 'red' edge shifts slowly toward the shorter wavelength, as shown in Fig. 4(a). Moreover, it can be seen from Fig. 5 that Δn_- is smaller in even-numbered bandgaps (gap 2) compared to odd-numbered bandgaps (gap 1) as a result from the higher floor in the gap 2. Hence, as shown in Fig. 4, the shallower even-numbered windows are more susceptible to bend loss [13,14].

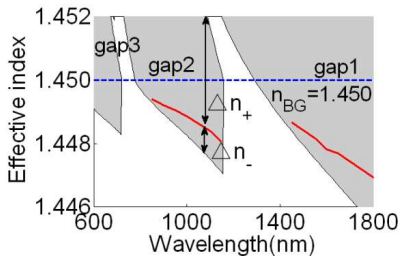


Fig. 5. Bandgap structure (grey region) and effective index (red curve) of the core mode in the PCF in which all air holes are fully filled by a fluid with a refractive index of 1.480, where Δn_- and Δn_+ illustrates respectively the downward and upward effective index mismatches between the core mode and the bands; the dash line illustrates the background pure silica index $n_{BG} = 1.450$.

Light could be guided in a hybrid PCF, e.g. a half-filled PCF, by the index- or bandgap-guiding mechanisms, depending on which of the two guiding mechanisms is predominate in the fiber [27]. Moreover, the mode distribution in the bent fiber will shift toward the outside of the bend due to the opposite index changes on the inside and outside of the bent fiber, resulting from the elasto-optic effect of the materials. Hence, while our half-filled PCF was bent toward the ‘180°’ orientation, the mode distribution shifted toward the filled-hole side so that the bandgap-guiding was predominate in the fiber. Consequently, as shown in Figs. 4(d) and 4(e), the bend loss occurs mainly in the ‘blue’ edge of the low-loss windows so that the bandgap narrowed with increased bend radius, as discussed above. On the contrary, while our half-filled PCF was bent toward the ‘0°’ orientation, the mode distribution shifted toward the unfilled-hole side so that the index-guiding was predominate in the fiber. Consequently, as shown in Figs. 4(b) and 4(d), the bandgaps were hardly affected because the index-guiding PCF was robust to the bending due to the significantly higher effective index mismatches between the core mode and the air hole cladding modes. While the half-filled PCF was bent toward the ‘90°’ or ‘270°’ orientation, the effect of the bending on the bandgaps was in an intermediate situation of the two cases above, as shown in Figs. 4(c), 4(d), and 4(f).

5. Conclusion

The bandgap edges of the half-filled PCF have distinct bend-sensitivities when the fiber is bent toward different fiber orientations. Especially, the transmission spectrum of the half-filled PCF is hardly affected by the bending to the filled-hole side. In other words, the bending properties of the half-filled PCF strongly depend on the bending orientations of the fiber. Such unique bend properties could be used to monitor simultaneously the bending orientation and the curvature of the engineering structures, as reported in [28]. On the other hand, compared with the fully-filled PCF, the half-filled PCF has, in general, a lower bend-sensitivity and even is bend-insensitive at special fiber orientation, which is of advantage to the communication applications of the fluid-filled PCFs. The proposed technique can be used to fill selectively one or several different types of fluids into any desired air holes in a PCF by means of carving several grooves on different sides of the fiber. As a result, more unique transmission properties could be achieved in the selectively-filled PCFs. Hence such a technique provides an easy way to achieve desired transmission properties in a PCF.

6. Acknowledgments

This work was supported by the Hong Kong Special Administrative Region Government through a GRF grant PolyU5190/08E, a Marie Curie International Incoming Fellowship within the 7th European Community Framework Programme, and a Foundation for the Author of National Excellent Doctoral Dissertation of China.